J. Eng. Technol. Sci., Vol. 53, No. 6, 2021, 210605

Noise Attenuation of a Duct-resonator System Using Coupled Helmholtz Resonator - Thin Flexible Structures

Iwan Prasetiyo[1,*], Gradi Desendra[1], Khoerul Anwar[1,2] & Mohammad Kemal Agusta[1]

[1]Engineering Physics, Faculty of Industrial Technology, Institut Teknologi Bandung
Jalan Ganesa 10, Bandung 40132, Indonesia
[2]National Research and Innovation Agency, Kawasan Puspiptek, Setu,
Tangerang Selatan, Banten, 15314, Indonesia
*E-mail: i.prasetiyo@fti.itb.ac.id

Highlights:

- The inclusion of a membrane can produce another peak along with the peak produced by the Helmholtz resonator so that the overall attenuation improves.
- The attenuation bandwidth is hardly to extend due to each peak being separated and not overlapping, which suggests that parameter selection should be done with great care.
- The peak attenuation of the membrane is tunable by changing its material properties.

Abstract. Several studies have been devoted to increasing the attenuation performance of the Helmholtz resonator (HR). One way is by periodic coupling of HRs in a ducting system. In this study, we propose a different approach, where a membrane (or a thin flexible structure in general) is added to the air cavity of a periodic HR array in order to further enhance the attenuation by utilizing the resonance effect of the membrane. It is expected that three attenuation mechanisms will exist in the system that can enhance the overall attenuation, i.e. the resonance mechanism of the HR, the Bragg reflection of the periodic system, and the resonance mechanism of the membrane or thin flexible structure. This study found that the proposed system yields two adjacent attenuation peaks, related to the HR and the membrane respectively. Moreover, extension of the attenuation bandwidth was also observed as a result of the periodic arrangement of HRs. With the same HR parameters, the peak attenuation by the membrane is tunable by changing its material properties. However, such a system does not always produce a wider attenuation bandwidth; the resonance bandwidths of both mechanisms must overlap.

Keywords: *acoustic attenuator; Bragg reflection; duct system; Helmholtz resonator; periodic structure; membrane; thin flexible structure.*

1 Introduction

Noise control at the low frequency regime is still a challenge, particularly for applications related to ductwork noise such as exhaust systems [1] and ventilation systems [2]. Typical sound attenuations in duct systems can be in the form of

Received October 6th, 2020, Revised May 24th, 2021, Accepted for publication July 8th, 2021.
 ISSN: 2337-5779,
DOI: 10.5614/j.eng.technol.sci.2021.53.6.5

resistive and reactive components. Reactive components are preferable over resistive components for low frequencies. However, such a system suffers from a relatively narrow attenuation bandwidth. To deal with this it is attractive to apply a periodic Helmholtz resonator (HR) system. It is evident that such a configuration can provide better attenuation benefitting from coupled Bragg reflection and HR resonance [3,4].

A periodic HR system is expected to be able produce even better performance, e.g. wider attenuation performance, more uniform attenuation, and so on. Hence, several studies have been conducted to enhance the performance of such systems. The enhancement can be in the form of the usage of multiple Helmholtz resonators with different tuning frequencies [5,6], coupling of the bandgap frequencies and the resonant frequency [7], and other improvements related to widening the bandwidth of the attenuation [8-11]. All the proposed configurations have shown improvement in terms of attenuation amplitude and bandwidth, where an improvement of 5-20 dB can be obtained. However, the number of HRs and the technique applied in these configurations can limit their application due to space requirements while the space may be limited in practice.

The use of membranes is another attractive option in noise control, since structural-acoustic coupling can produce attenuation [12,13]. In the context of duct systems this can be interaction between a flexible structure and the sound field in the duct, which is highly dependent on the modal characteristic of the structure and acoustic cavity [14]. Satisfactory attenuation in a silencer can be achieved at low to mid frequency when the membrane properties are properly chosen [15-17]. Recently, such membranes have been widely applied in acoustic meta materials (AMMs) to exploit the band gap structure for better attenuation and absorption at low frequencies [18-22].

This work aimed to demonstrate that additional attenuation can be obtained from the use of a membrane (or a thin flexible structure in general) as resonator element embedded in a periodic HR system. This can enhance overall attenuation due to the presence of multiple resonance, while space can be saved to accommodate practical constraints. A simple theoretical approach is provided to verify its behaviors under $\boldsymbol{kd} \ll \mathbf{1}$ condition, where such a system is mounted on a one-dimensional duct. Hence, a single degree of freedom mass-spring model for a Helmholtz resonator in a duct coupled with the Bloch theorem is applicable. Moreover, experiments were conducted on a similar system by developing samples by means of modular 3D printing with variation of membrane properties. The remainder of this paper is divided into four sections. In Section 2, a theoretical formulation of the proposed system is provided, followed by an explanation of the experimental system in Section 3. The obtained results are

discussed in Section 4 and finally the most important findings are outlined in Section 5.

2 Theoretical Formulation

2.1 Single Cell

A schematic of an HR mounted on a duct is shown in Figure 1. p_1 and p_2 define the pressure at the duct-neck interface while u_1 and u_2 are attributed to the particle velocity in the same area. The continuity condition of pressure and volume velocity at the interface of the duct-neck suggest: (1) $p_1 = p_2$; (2) $S_d u_1 = S_d u_2$. Hence, the relationship of the acoustic parameters at point 1 and 2 can be expressed as follows [23]:

$$\begin{bmatrix} p_1 \\ \rho_0 c_0 u_1 \end{bmatrix} = \begin{bmatrix} 1 & 0 \\ \rho_0 c_0 / S_d Z_r & 1 \end{bmatrix} \begin{bmatrix} p_2 \\ \rho_0 c_0 u_2 \end{bmatrix} \tag{1}$$

where ρ_0 is the air density, c_0 is the speed of sound in air, and S_d is the cross-section area of the duct. Meanwhile, Z_r is the surface impedance of the Helmholtz resonator, defined as [24]:

$$Z_r = r_{hr} + j\underbrace{(\omega \frac{\rho_0 l'_n}{S_n}}_{Z_{r1}} \underbrace{- \frac{1}{\omega} \frac{\rho_0 c_0^2}{V_r})}_{Z_{rc}} \tag{2}$$

where r_{hr} is the acoustic resistance of HR, S_n is the cross-section area of the HR's neck, $l'_n = l + 0.85d$ is the effective length of the HR's neck, and V_r is the volume of the HR's air cavity. The real part of Z_r is related to the visco-thermal effect that is present in the HR's neck while the imaginary part is related to the total mass of the neck and the stiffness of the air cavity.

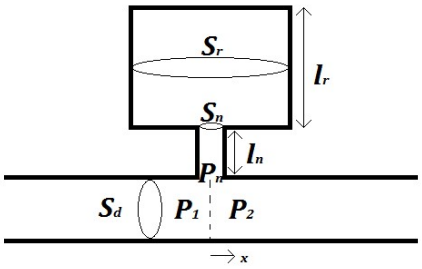

Figure 1 Schematic of a duct with a single-cell HR.

In this study, a membrane (or a thin flexible structure) was then added to the air cavity of the HR, as illustrated in Figure 2. The associated impedance is expressed as follows [12]:

$$Z_m = r_m + j[\underbrace{\omega m'}_{Z_{m1}} - \underbrace{\rho_0 c_0 \cot(kd)}_{Z_{mc}}] \tag{3}$$

where r_m is the acoustic resistance of the membrane, m' is the mass of the membrane, and d is the depth of the air cavity. Eq. (3) reflects that the real part of Z_m is the damping quotient that is governed by the membrane material, while the imaginary part is related to the mass of the membrane and the stiffness of the backing air cavity of the membrane. Practically, the stiffness can be adjusted by changing the position of the membrane as the air cavity acts as a spring in this model.

A schematic of the HR with a membrane inside the air cavity can be seen in Figure 2(a). The interaction between the resonator and the membrane can be modeled using the electro-acoustic equivalent approach, where the damping factors from the resistance factor are omitted, which is acceptable for the case of non-sub-millimeter holes. Moreover, the fundamental mode is the only mode considered, which is acceptable for low frequencies. Apart from this, such a model is considered to be useful for initial investigation of the proposed resonator system. The imaginary parts of Eqs. (2) and (3) tend to zero when the system resonates, from which the resonance frequency can be obtained accordingly.

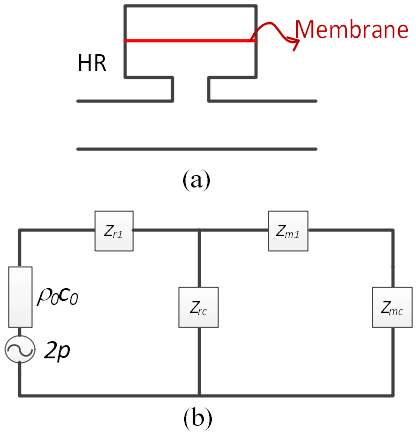

Figure 2 (a) Helmholtz resonator with membrane, (b) electro-acoustic equivalent model of coupled Helmholtz resonator and membrane.

The combination of an HR and a membrane was modeled using an equivalent electro-acoustic circuit, as shown in Figure 2(b), yielding the effective impedance Z_{rm} as follows:

$$Z_{rm} = j\omega\frac{\rho_0 l_n'}{S_n} + \frac{\left(2m'\rho_0 c_0^2/V_r\right) + \left(2\rho_0^2 c_0^3/\omega V_r\right)\cot(k\,l_r/2)}{j\left[\left(\omega m' - \rho_0 c_0\cot(k\,l_r/2)\right) - 2\rho_0 c_0^2/\omega V_r\right]} \tag{4}$$

where $d = l_r/2$ for a membrane situated in the middle of the air cavity.

Considering the four pole parameters indicated in Eq. (1), the resulting attenuation of the duct with one HR can be evaluated in terms of the transmission loss (TL) as follows [1,23]:

$$TL = 20\log_{10}\left(\frac{1}{2}\left|2 + \frac{\rho_0 c_0}{S_d}\frac{1}{Z_{rm}}\right|\right) \tag{5}$$

2.2 Periodic Cell

A schematic of the periodic system of the Helmholtz resonator array is presented in Figure 3.

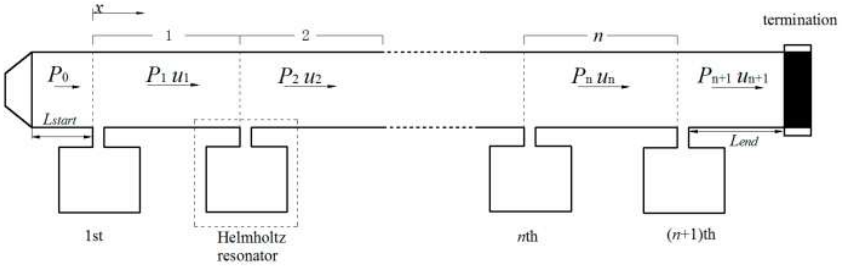

Figure 3 Schematic of the duct with a periodic Helmholtz resonator array.

For the case of a periodic cell, the pressure field can be expressed as a combination of a right-going and a left-going plane wave with unknown amplitude. By introducing a continuity condition of pressure and volume velocity at the duct-neck interface at $x = nl_d$, a linear 2×2 algebraic system relating the incoming and outgoing plane wave amplitude can be obtained as follows:

$$\begin{bmatrix} C_{n+1}^{+} \\ C_{n+1}^{-} \end{bmatrix} = \mathbf{T}\begin{bmatrix} C_{n}^{+} \\ C_{n}^{-} \end{bmatrix} \tag{6}$$

with

$$\mathbf{T}=\begin{bmatrix}\left(1-\dfrac{S_n\rho_0c_0}{2S_dZ_{rm}}\right)e^{-jkl_d} & -\dfrac{1}{2}\dfrac{S_n\rho_0c_0}{S_dZ_{rm}}e^{jkl_d}\\ \dfrac{1}{2}\dfrac{S_n\rho_0c_0}{S_dZ_{rm}}e^{-jkl_d} & \left(1+\dfrac{S_n\rho_0c_0}{2S_dZ_{rm}}\right)e^{jkl_d}\end{bmatrix}$$

However, multiplication of the transfer matrix in Eq. (6) with an identical matrix does not account for the attenuation effect from the periodicity. Therefore, the Bloch theorem is used instead to model the periodicity-induced attenuation, which can be expressed as follows [3]:

$$\begin{bmatrix}C_{n+1}^{+}\\ C_{n+1}^{-}\end{bmatrix}=e^{-jql_d}\begin{bmatrix}C_{n}^{+}\\ C_{n}^{-}\end{bmatrix} \tag{7}$$

where q is the Bloch wavenumber and l_d is the lattice distance or the distance between two successive HRs.

The Bloch wavenumber can have a complex value that includes a real part and an imaginary part. The analysis of this can be obtained by setting $\lambda = e^{-jql_d}$ so that the solution of the periodic cells or the HR array can be broken down into the solution of the eigenvalue and the associated eigenvectors. There are two general solutions for $\lambda = \lambda_1$ and λ_2 respectively with corresponding eigenvectors for each eigenvalue $[v_{I1}, v_{R1}]^T$ and $[v_{I2}, v_{R2}]^T$. Hence, Eq. (7) can be written as

$$\begin{bmatrix}C_{n+1}^{+}\\ C_{n+1}^{-}\end{bmatrix}=\mathbf{T}^n\begin{bmatrix}C_{n}^{+}\\ C_{n}^{-}\end{bmatrix}=A_0\lambda_1^n\begin{bmatrix}v_{I1}\\ v_{R1}\end{bmatrix}+B_0\lambda_2^n\begin{bmatrix}v_{I2}\\ v_{R2}\end{bmatrix} \tag{8}$$

The averaged transmission loss for n cells can be written as follows:

$$\overline{TL}=\frac{20}{n+1}\log_{10}\left|\frac{C_0^{+}}{C_{n+1}^{+}}\right|=\frac{20}{n+1}\log_{10}\left|\frac{A_0\lambda_1^{-1}v_{I1}+B_0\lambda_2^{-1}v_{I2}}{A_0\lambda_1^{n}v_{I1}+B_0\lambda_2^{n}v_{I2}}\right| \tag{9}$$

where $\overline{TL}$ defines the averaged transmission loss for n HR cells, A_0&B_0 defines the complex constants of the wave propagation, λ_1^n and λ_2^n define the eigenvalue of the propagation matrix in the n^{th} cell and v_{I1} and v_{I2} define the characteristic vectors of the wave propagation. The eigenvalue λ describes the dispersion relation of the propagating wave, where the real part of the dispersion relation defines the amplitude of the attenuation and the imaginary part of the dispersion relation defines the frequency band where the sound may or may not propagate. Eq. (9) defines the attenuation performance of the periodic system of a coupled Helmholtz resonator and membrane. Theoretically, a number of HRs greater than five will not produce a significant improvement of the attenuation. For this reason, the number of HRs in the experimental work was limited to five.

It should be noted that a strong coupling between the Bragg reflection and the resonator exist when the relationship $l_d = \frac{1}{2}\lambda$ is satisfied, where λ is the operating sound wavelength of the resonator. Under such a circumstance, the Bragg reflection's frequency coincides with the designed resonance frequency of the HR. This can be beneficial to obtaining a broader attenuation bandwidth, as indicated in Figure 4. Otherwise, the broader attenuation cannot be maximized without the coupling effects of the HR's resonance and the Bragg reflection, as found from five HRs with $l_d = 10$ cm or $l_d = 20$ cm.

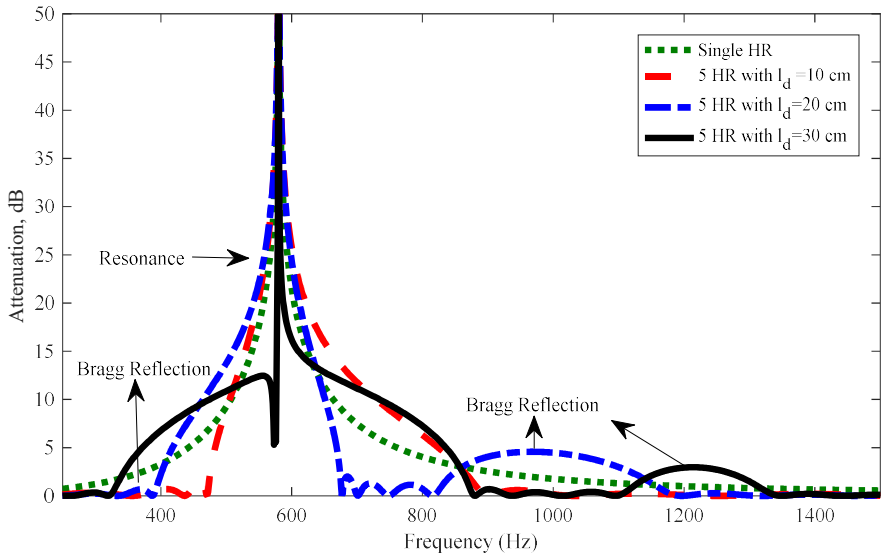

Figure 4 Attenuation band of periodic HR array due to Bragg reflection and HR resonance.

3 Experimental System

3.1 Sample Development

The basic structure consisted of a single-cell HR made of polylactic acid (PLA) by means of a 3D printer, as shown in Figure 5. The single-cell HR had a resonator neck length of 4 cm, a resonator neck diameter of 3.4 cm and the volume of the air cavity was around 100.5 cm^3 unless otherwise stated. With these dimensions, the resonance frequency was expected to be around 580 Hz. Moreover, to ensure the cells were tightly connected, adhesive tape was applied to the joints. To enable placing the membrane, the air cavity of the single-cell HR

consisted of two different parts, designated as the upper body and the lower body respectively, while the membrane was stretched across the cross section of the air cavity. Hence, the membrane was held by the upper and the lower body accordingly. In this study, three different membranes were used, as listed in Table 1, while only the mass of the membrane was considered in the model.

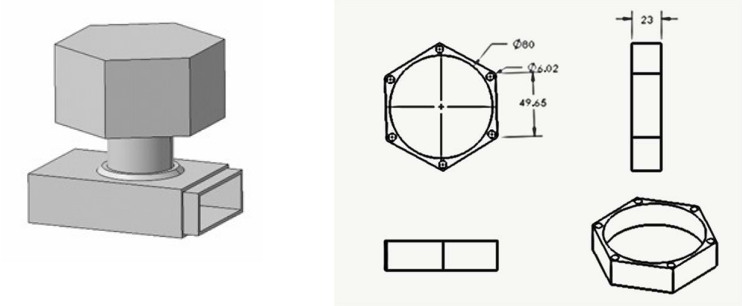

Figure 5 Basic construction of a single-cell HR and associated cross-section shape.

Table 1 Material properties of the membrane and thin flexible panel used in the system.

Material	Thickness (mm)	Density (gr/mm^2)	m'
Rubber	1.0	1.60 ×10^{-3}	318.31
Denim fabric	0.6	0.52 ×10^{-3}	103.62
Aluminum foil	0.1	0.25 ×10^{-3}	49.74

3.2 Experimental Setup

Figure 6 presents the measurement schematic. The measurements were conducted in an anechoic chamber with a 1/4" omni-directional microphone, while a 5.5-cm driver speaker was used to generate white noise plane waves in order to obtain the insertion loss (*IL*) as a performance indicator. This differs from transmission loss (*TL*) measurement in that it needs anechoic termination and a more complex configuration. The measurements were repeated twice for each sample to collect data from the configuration with and without HR system. Apart from that, IL and TL are comparable for evaluating attenuation performance of duct attenuation [1]. Following ISO-10534, the upper frequency limit (f_u) was determined by $f_u d < 0.5 c_0$, where d is the largest dimension of the tube cross section and c_0 is the wave speed. With d = 60 mm it was found that f_u was around 2850 Hz. Meanwhile, the lower frequency limit was determined by the hardware specification and the loudspeaker response, where the hardware used in this experiment was capable of registering measurements as low as 100 Hz. Considering this, the measurement frequency was expected to be valid from 250

Hz to 2000 Hz and the corresponding data were collected using a real-time analyzer. Moreover, to ensure sufficiency of the signal-to-noise ratio (SNR) measurement, the SPL difference of the background noise and the receiver point was kept to exceed 15 dB.

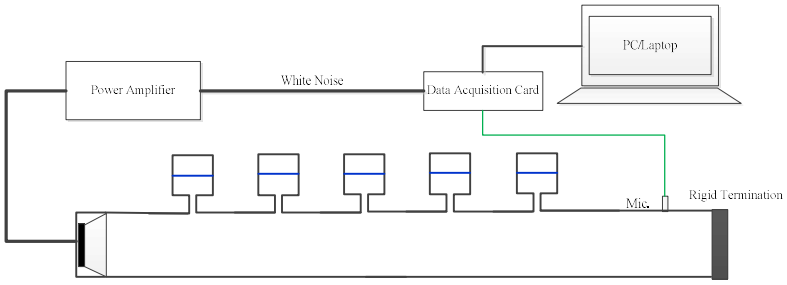

Figure 6 Measurement schematic of the Helmholtz resonator array.

The actual overall system of the measurement setup can be seen in Figure 7. To obtain single-cell HR measurements, the other four resonators and four blocks on the duct were removed. The periodic or lattice distance was set to 10 cm rather than 30 cm as the ideal distance due to sample fabrication constraints of the 3D printer. Moreover, this work was devoted to investigating the benefit of membrane inclusion in a periodic HR system rather than investigating the periodic system itself. Hence, the experimental set up should be sufficient to satisfy this purpose.

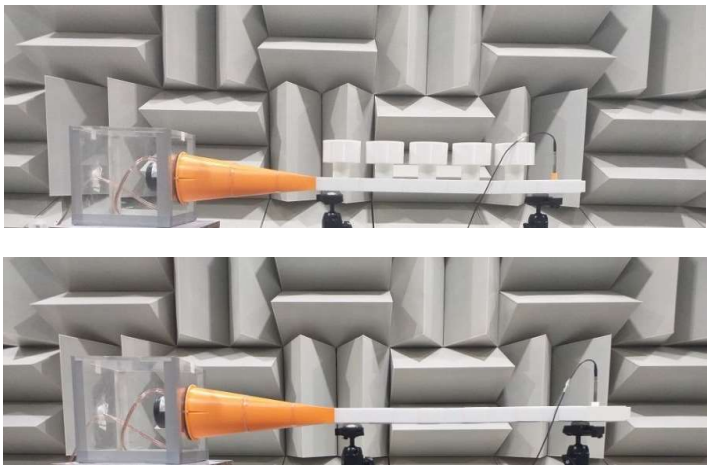

Figure 7 Actual configuration of the system, where the resonators are present (top) and duct only (bottom) to obtain the *IL* of the resonator system.

4 Results and Discussions

4.1 System without Membranes

The *IL* behavior of a single-cell HR and a five-cell HR can be seen from Figure 8. The measurement result indicates that the maximum attenuation occurred at 563 Hz with an amplitude of around 15 dB, as shown in Figure 8(a).

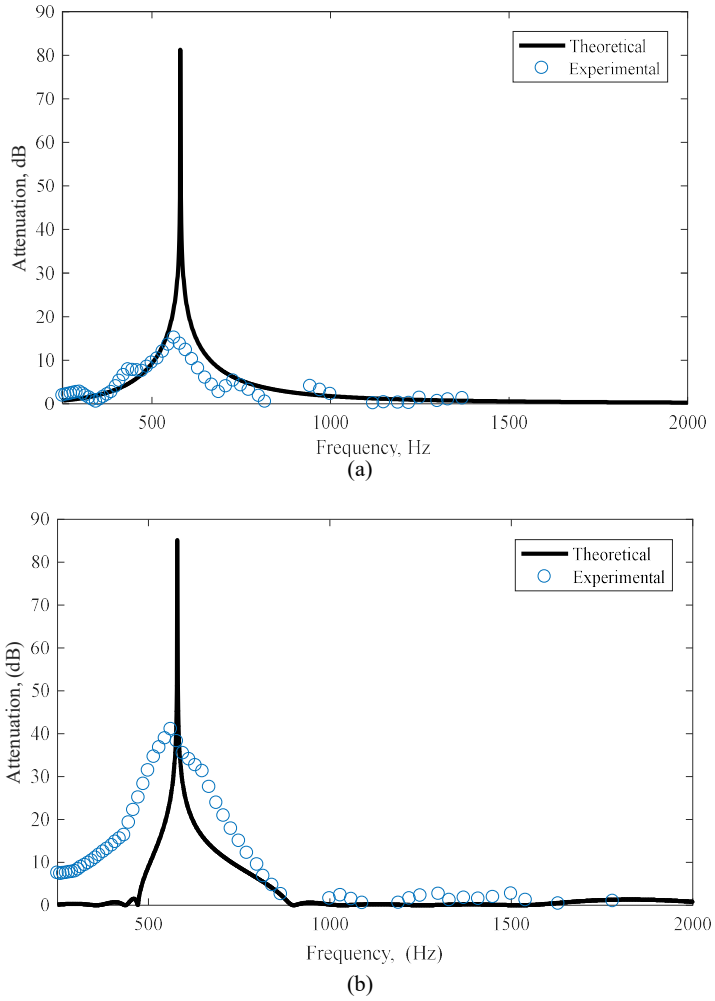

Figure 8 Attenuation comparison of theoretical and experimental result: (a) single-cell HR; (b) 5-cell HR.

Compared to the theoretical result, the corresponding resonance frequency deviated about 17 Hz, while the amplitude had a difference of around 66 dB. This can be attributed to characteristic losses, which may be affected by small fabrication defects or surface roughness from 3D printing. Moreover, the bandwidth difference between the results was also pronounced around 43 Hz. Apart from this, the overall behaviors of both HRs were comparable. As expected, the attenuation level and the bandwidth improvements are evident for the five-cell HR, as can be seen in Figure 8 (b). The attenuation of the five-cell HR was around 41 dB, where it was only 15 dB for the single-cell HR, while the bandwidth increased from 228 Hz to 568 Hz. The discrepancies between the theoretical and the experimental results for this case tended to increase. This may be related to defect accumulation from each of the HRs. However, in general, the comparison result is reasonable, where both indicate a similar resonance frequency as well as bandwidth extension.

4.2 System with Membranes

With inclusion of a membrane it is expected that more peaks will be present from the HR system. Such behavior can be observed in Figure 9 where a fabric membrane was used. It was found that an additional peak due to the inclusion of a membrane was present in both the single-cell HR (see Figure 9(a)) and the five-cell HR case (see Figure 9(b)), while the experimental results showed similar behavior.

Compared to the single-cell HR case, the extension of bandwidth around the resonance frequency also existed in the five-cell HR case, which is due to more resonators being involved while the coupling effect of Bragg reflection and HR resonance on the bandwidth was small due to the use of a non-optimal lattice distance. It can also be seen that a resonance frequency shift occurred for the periodic coupled HR-membrane system, where a difference of 133 Hz was present for the 1st peak compared with a periodic HR system only. This is presumably due to the interaction between the Helmholtz resonator and the corresponding membrane modes. Moreover, the theoretical result indicates that the attenuation of the coupled HR-membrane system was distributed over a wider frequency but the attenuation bandwidth of the periodic HR system (see the 1st peak attenuation) was reduced compared to that of the system without membrane. However, there is potential to have more attenuation due to higher membrane modes as indicated by the experimental results, while only the fundamental mode was considered in the theoretical result. Hence this behavior was absent from the theoretical result.

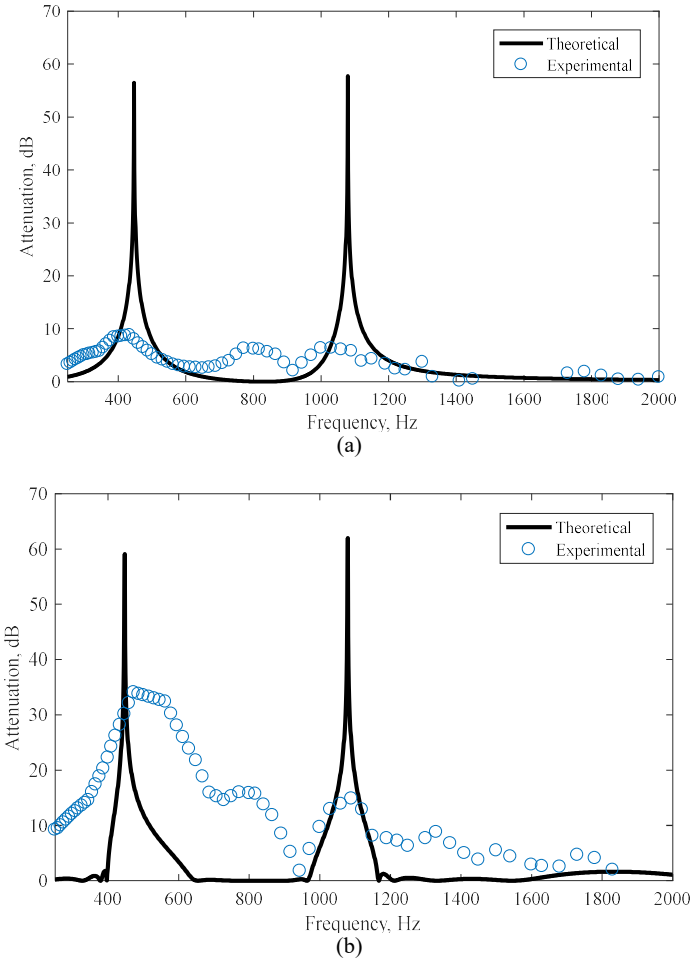

Figure 9 Attenuation comparison of theoretical and experimental result for Helmholtz resonator with membrane: (a) single-cell HR; (b) five-cell HR.

The comparison of the theoretical and the measurement result showed that the attenuation amplitude around the resonance frequency had discrepancies. Moreover, the attenuation bandwidth of the measurement result tended to be wider than the predicted one. However, this behavior was present even for the periodic HR system so that the same reason holds. There are several possible explanations for these discrepancies. One is related to multi-mode interaction between the air cavity and the membrane. Another one is related to the damping component that was omitted from the model. Apart from that, both results

indicate similar behavior in terms of the presence of additional peaks and attenuation improvement for the periodic HR system. Overlapping attenuation did not occur between the two peaks so that extending of the overall attenuation bandwidth could not be constructed. Apart from this, additional peaks could be obtained from the proposed structure rather than from the original HR structure.

4.3 Influence of Membrane Properties on Attenuation Characteristics

It is instructive to observe the attenuation behavior for different membrane properties from the measurement results. It should be noted that the specification of the HR and the position of the membrane in the air cavity were kept the same. It can be seen from Figure 10 that peak attenuation of a periodic HR with a fabric membrane existed around 473 Hz and 1090 Hz. Meanwhile, a prominent peak around 688 Hz was present for the case of an aluminum foil membrane.

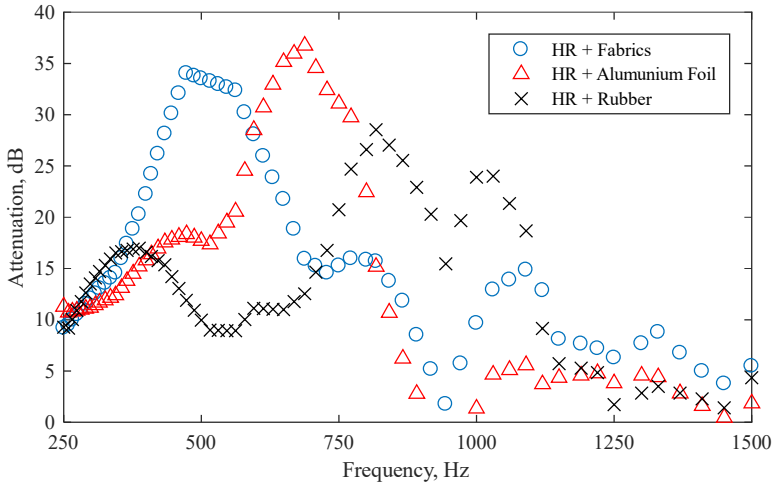

Figure 10 Comparison of attenuation characteristics of periodic HRs with different membrane properties.

For the case of a rubber membrane, the peaks were pronounced around 370 Hz and 800 Hz. Although the HRs had the same specification, none of them produced identic resonance peaks. These results indicate that interaction of the HR mode and the membrane mode can shift the original resonance frequency of each element and that such a condition at least affects the HR resonance frequency. Apart from this, it is useful to take the properties of the membrane into account when tuning the desired attenuation at a particular frequency. Hence, selection of the membrane properties must be done with a great care.

5 Conclusions

The inclusion of a membrane into a Helmholtz resonator array was studied. It was found that the membrane could produce additional attenuation apart from the attenuation due to the HR resonance and the Bragg reflection. This was confirmed by the experimental results. It was also found that the attenuation of the membrane could be tuned at a particular frequency by changing its material properties. Despite this, attenuation bandwidth extension as a result of membrane inclusion cannot be easily obtained; overlapping attenuation must be present. For this, further study is required to determine suitable membrane properties and configurations.

Acknowledgement

This research is supported by the Institute of Research and Community Service of Institut Teknologi Bandung (LPPM ITB), under the P3MI 2019 research scheme, with the contract number 0922c/I1.C06.2/PL/2019.

References

[1] Munjal, M., *Acoustics of Ducts and Mufflers*, New York: Wiley, 1987.
[2] De Salis, M.H.F., D.J. Oldham, D.J. & Sharples, S., *Noise Control Strategies for Naturally Ventilated Buildings*, Building and Environment, **37**(5), pp. 471-484, 2002.
[3] Bradley, C.E., *Time Harmonic Acoustic Bloch Wave Propagation in Periodic Waveguides. Part I. Theory*, The Journal of the Acoustical Society of America, **96**(3), pp. 1844-1853, 1994.
[4] Chen, K.T., *The Improvement on The Transmission Loss of a Duct by Adding Helmholtz Resonator*, Applied Acoustics, **54**(1), pp. 71-82, 1998.
[5] Romero-García, V., *Use of Complex Frequency Plane to design Broadband and Sub-Wavelength Absorbers*, The Journal of the Acoustical Society of America, **139**(6), pp. 3395-3403, 2016.
[6] Wu, D., *Hybrid Noise Control Using Multiple Helmholtz Resonator Arrays*, Applied Acoustics, **143**, pp. 31-37, 2019.
[7] Wang, X. & Mak, C.M., *Disorder in a Periodic Helmholtz Resonators Array*, Applied Acoustics, **82**, pp. 1-5, 2014.
[8] Seo, S.H. & Kim, Y.H., *Silencer Design By Using Array Resonators for Low-Frequency Band Noise Reduction*, The Journal of the Acoustical Society of America, **118**(4), pp. 2332-2338, 2005.
[9] Li, D. & Cheng, L., *Acoustically Coupled Model of an Enclosure and a Helmholtz Resonator Array*, Journal of Sound and Vibration, **305**(1), pp. 272-288, 2007.

[10] Wang, X. & Mak, C.M., *Wave Propagation in a Duct with a Periodic Helmholtz Resonators Array*, The Journal of the Acoustical Society of America, **131**(2), pp. 1172-1182, 2012.
[11] Cai, C. & Mak, C.M., *Acoustic Performance of Different Helmholtz Resonator Array Configurations*, Applied Acoustics, **130**, pp. 204-209, 2018.
[12] Cox, T.J. & D'Antonio, P., *Acoustic Absorbers and Diffusers: Theory, Design and Application*, London: Taylor and Francis, 2009.
[13] Morse, P.M. & I. K.U., *Theoretical Acoustics*, New York: McGraw-Hill, 1968.
[14] Fahy, F. & Gardonio, P., *Sound and Structural Vibration: Radiation, Transmission and Response*, New York: Academic; 2007, UK: Academic Press, 1985.
[15] Du, J., Y. Liu, Y. & Zhang, Y., *Influence of Boundary Restraint on Sound Attenuation Performance of a Duct-Membrane Silencer*, Applied Acoustics, **105**, pp. 156-163, 2016.
[16] Liu, Y. & Du, J., *Sound Attenuation Analysis and Optimal Design for A Duct with Periodic Membranes Embedded in its Sidewalls*, Journal of Applied Physics, **125**(3), 034901, 2019.
[17] Ramamoorthy, S., Grosh, K. & Nawar, T.G., *Structural Acoustic Silencers-Design and Experiment*, The Journal of the Acoustical Society of America, **114**(5), pp. 2812-2824, 2003.
[18] Huang, T.Y., Shen, C. & Jing, Y., *Membrane- and Plate-Type Acoustic Metamaterials*, The Journal of the Acoustical Society of America, **139**(6): pp. 3240-3250, 2016.
[19] Wang, X., *Membrane-Constrained Acoustic Metamaterials for Low Frequency Sound Insulation*, Applied Physics Letters, **108**(4), 041905, 2016.
[20] Zhao, J., *Membrane-Type Acoustic Metamaterials with Tunable Frequency by a Compact Magnet*, The Journal of the Acoustical Society of America, **145**(5), pp. EL400-EL404, 2019.
[21] Lu, Z., *Membrane-Type Acoustic Metamaterial with Eccentric Masses For Broadband Sound Isolation*, Applied Acoustics, **m157**, 107003, 2020.
[22] Langfeldt, F. & Gleine, W., *Membrane- and Plate-Type Acoustic Metamaterials with Elastic Unit Cell Edges*, Journal of Sound and Vibration, **453**, pp. 65-86, 2019.
[23] Ji, Z. & Sha, J., *Four-pole Parameters of a Duct with Low Mach Number Flow*, The Journal of the Acoustical Society of America, **98**(5), pp. 2848-2850, 1995.
[24] Ingard, U*., On the Theory and Design of Acoustic Resonators,* The Journal of the Acoustical Society of America, **25**(6), pp. 1037-1061, 1953.